

Reduced Jet-Medium Coupling in Pb+Pb Collisions at the LHC?

Barbara Betz and Miklos Gyulassy

Department of Physics, Columbia University, New York, 10027, USA

The nuclear modification factor, R_{AA} , of jet fragments in 2.76 ATeV Pb+Pb collisions observed by the ALICE and CMS Collaborations at the Large Hadron Collider (LHC) suggests that the Quark-Gluon Plasma (QGP) may be less opaque to jets than expected from fixed jet-medium coupling extrapolations from the Relativistic Hadron Collider (RHIC). We evaluate the effective reduction factor of the jet-medium coupling from a combined fit to the available data on $R_{AA}(\sqrt{s}, p_T, b)$ and the elliptic flow $v_2(\sqrt{s}, p_T, b)$ at $\sqrt{s} = 0.2, 2.76$ ATeV in the transverse momentum range $p_T \sim 5 - 100$ GeV and a broad centrality (impact parameter, b) range. We compare Glauber and Color Glass Condensate (CGC) initial conditions using a simple analytic energy-loss model ($dE/dx = -\kappa E^a x^z T^{z-a+2}$) that can interpolate between weakly-coupled tomographic and strongly-coupled holographic jet energy-loss models. Extrapolation from RHIC to LHC assuming a fixed jet-medium coupling, κ , and a monotonic density dependence, leads to an overquenching of R_{AA} at LHC for both Glauber and CGC initial conditions and both $z = 1, 2$ path-length dependencies. The fit to the p_T and centrality dependence of R_{AA} at LHC requires a reduced coupling $\kappa_{LHC} \approx (0.6 \pm 0.1) \kappa_{RHIC}$ with either initial geometry and either path-length dependence. Interpreted in terms of weakly-coupled jet tomography, this implies a modest reduction of $\alpha_{LHC} \approx 0.9 \alpha_{RHIC}$ at temperatures $T_{LHC} \approx 1.3 T_{RHIC}$. However, in terms of strongly-coupled gravity dual holography, the fit implies a more rapid reduction of the effective t'Hooft coupling, $\lambda_{LHC} \sim 0.5 \lambda_{RHIC}$. Surprisingly, unlike at RHIC, the preliminary LHC data on the high- p_T $R_{AA}(p_T, b)$ appears to be inconsistent with CGC initial geometries.

I. INTRODUCTION

First data from the Large Hadron Collider (LHC) on the nuclear-size dependence of jet-medium interactions in Pb+Pb collisions at $\sqrt{s} = 2.76$ ATeV [1–14] suggest that the Quark-Gluon Plasma (QGP) may be less opaque than expected [15–18] from the factor of two increase in the bulk charged-particle multiplicity per unit rapidity, $dN_{ch}/d\eta$, relative to the $\sqrt{s} = 0.2$ ATeV measured value at the Relativistic Heavy Ion Collider (RHIC) [19–23].

One of the interesting open questions at RHIC is whether jet-medium interactions in dense deconfined QGP-matter can be better described in terms of weakly-coupled perturbative QCD (pQCD) tomography or novel strongly-coupled gravity-dual Anti-de-Sitter/Conformal Field Theory (AdS/CFT) string-model holography [24, 25]. The first data from LHC provide new tests for jet-medium interaction models in a QGP density range that extends the range accessible at RHIC. Doubling the QGP density, corresponding to a 30% increase of temperature relative to RHIC, required the factor of ten increase in the center-of-mass energy per nucleon.

In order to extract either tomographic or holographic information from the jet-quenching observable systematics, it is important to have a well calibrated initial jet-flux and an initial jet-production-point geometry. Two competing models, the Glauber [26] and the Color Glass Condensate (CGC) [27], have been used so far to predict the impact parameter b and beam energy \sqrt{s} of those distributions as well as the initial QGP medium geometry. The Glauber model is based on an eikonal Wood-Saxon nuclear geometry and assumes incoherent superposition of proton-proton collisions. The CGC model takes possible coherent small- x saturation effects [28–30]

into account. We consider both models below to gauge the magnitude of systematic theoretical errors associated with initial QGP geometries.

In this work, we use a simplified analytic jet-energy-loss model [31, 32] that generalizes the geometric absorption model used in Refs. [33–36] to compute both the nuclear modification factor R_{AA} and the elliptic flow v_2 for a variety of jet path-lengths and energy dependencies

$$\frac{dP}{d\tau}(\vec{x}_0, \phi, \tau) = -\kappa P^a(\tau) \tau^z T^{z-a+2}[\vec{x}_\perp(\tau), \tau] / (\hbar c)^{1+z}. \quad (1)$$

Here, the energy loss per unit length, $dE/dx = dP/d\tau$, is given as a function of proper time τ for a fixed jet rapidity y . The transverse jet path is $\vec{x}_\perp(\tau) = \vec{x}_0 + \hat{n}(\phi)\tau$ from the production point \vec{x}_0 in direction of an azimuthal angle ϕ relative to the reaction plane. The dimensionless effective medium coupling κ is proportional to α_s^3 in the case of radiative energy-loss tomography while it is proportional to $\kappa \propto \sqrt{\lambda_{tH}} \propto (\alpha_s N_c)^{1/2}$ in terms of the t'Hooft coupling at large N_c in case of gravity-dual holography. $T(\vec{x}, \tau)$ is the local temperature field of the QGP. As in Refs. [31, 32], we assume that the energy loss depends monotonically on the comoving local entropy density, $\sigma(\vec{x}, \tau) \propto T^3(\vec{x}, \tau) = T^3(\vec{x}, \tau_0) \tau_0 / \tau$, that decreases with τ as in ideal boost-invariant Bjorken hydrodynamics [45].

We note that the monotonic power-law dependence of dE/dx on the temperature (or entropy) field in Eq. (1) is a strong model assumption in this paper motivated by standard pQCD tomography and AdS/CFT holography models. As shown by Liao and Shuryak [37], non-monotonic ansatzes, e.g. magnetic monopole enhanced dE/dx near the critical QCD transition point, $T_c \approx 170$ MeV, may also be able to explain the (R_{AA}, v_2) -

correlations at RHIC and LHC, but at the price of additional dynamical parameters. We limit the scope of the present study to investigate whether a consistent account of RHIC and LHC (R_{AA}, v_2)-correlations can be achieved with a simpler monotonic density dependence of jet-medium interactions.

Note that $a \approx 1/3$ describes approximately both the pQCD and the AdS/CFT falling string cases. An $(E/T)^{1/3}$ energy dependence is numerically close to the logarithmic $\log(E/T)$ dependence predicted by pQCD energy loss in the range $10 < E/T < 600$ relevant up to LHC. This approximate power law is also consistent with the lower bound of a in the falling-string scenario in AdS/CFT holography [38, 39].

In our model, the parameters a, z control the jet-energy (momentum) and path-length dependence of jet-energy loss. Varying $z = 1$ to $z = 2$ allows us to interpolate between the weakly and strongly-coupled dynamical limits. Note that Eq. (1) reduces to the absorption model referred to as "AdS/CFT" in Refs. [33–35], which is independent of jet energy, for $a = 0, z = 2$. For $a = 1, z = 0$, on the other hand, the model reduces to the heavy-quark string-drag energy-loss of conformal AdS holography [38, 39]. Since for light quark and gluon jets the heavy-quark string-drag ($a = 1$) model does not apply, we use here instead ($a = 1/3, z = 2$) to characterize approximately off-shell falling-string AdS/CFT-holography with a Bragg-like end peak [38–42]. Recent work [43] on falling string energy-loss has identified important corrections to the original works [38, 39] that appears to reduce the path-length power-law dependence from $z = 2$ back to $z \approx 1$. Parametrically, this would make pQCD and AdS/CFT descriptions virtually indistinguishable for light jets. Below we will nevertheless compare both $z = 1$ and $z = 2$ cases to estimate systematic theoretical errors associated with different path-length possibilities.

In this work, we further generalize Ref. [31] by using the full pQCD jet-production p_T -spectra for quark and gluon jets instead of approximating those distributions via their spectral indices. In addition, we convolute the quenched jet spectra with KKP pion fragmentation functions [44].

As in Refs. [31, 32], we consider 1D-Bjorken expansion [45] with different initial starting values of $\tau_0 = 0.01, 1.0$ fm/c. The magnitude of the cube of the initial temperature profile is assumed to scale with the observed rapidity density $T_0^3(\vec{x}) \propto \rho(\vec{x}, b) dN_{ch}(\sqrt{s}, b)/d\eta$. The initial transverse coordinate distribution, $\rho(\vec{x}, b)$, of the QGP is modeled according to a Glauber or a CGC-like geometry [see Eqs.(10) and (11) below].

The high- p_T transverse Fourier moments, especially the elliptic flow, are sensitive to the early-time evolution and QGP formation era [17, 31, 32]. In particular, the conclusion drawn from Refs. [33, 34] that the measured data for $R_{AA}(N_{part})$ and $v_2(N_{part})$ at RHIC energies can best be described with CGC initial conditions and an AdS/CFT-like energy loss remain valid only under the assumption that the QGP formation time τ_0 is

set to zero, $\tau_0 \sim 0$ fm [31, 32]. However, for $\tau_0 = 1$ fm, as suggested from bulk-flow fits via hydrodynamics [46], both pQCD-like and AdS/CFT-like energy-loss models were shown in Ref. [32] to predict similar high- p_T R_{AA} as well as v_2 and to reproduce the data within current experimental errors.

In the case of an AdS/CFT-like energy-loss, an approximate quadratic path-length dependence $dE/dx \sim x^2$ leads to a suppression of energy loss for small path lengths and early times. Assuming that there is no appreciable energy loss within the first fm, both pQCD and AdS/CFT-like energy-loss models predict similar nuclear modification factors and elliptic moments at high- p_T , once the jet-medium coupling is adjusted to fit the most central nuclear modification factor at a single reference p_T as we show below.

II. A GENERIC JET-QUENCHING MODEL

The nuclear modification factor R_{AA} is the ratio of jets in the QGP to jets in vacuum (here we omit an obvious N_{part} dependence for the sake of readability),

$$R_{AA}^{q,g}(P_f, \vec{x}_0, \phi) = \frac{dN_{QGP}^{jet}(P_f)}{dyd\phi dP_f^2} \bigg/ \frac{dN_{vac}^{jet}(P_f)}{dyd\phi dP_0^2} \\ = \frac{dP_0^2}{dP_f^2} \frac{dN_{vac}^{jet}[P_0(P_f)]}{dyd\phi dP_0^2} \bigg/ \frac{dN_{vac}^{jet}(P_f)}{dyd\phi dP_0^2}. \quad (2)$$

Denoting the invariant jet distribution $g_0(P)$ as

$$g_0(P) = \frac{dN_{vac}^{jet}(P)}{dyd\phi dP^2}, \quad (3)$$

the nuclear modification factor for a quark (q) or gluon (g) jet with a final momentum P_f , produced at transverse coordinate \vec{x}_0 , and propagating in direction ϕ is, from Eq. (1),

$$R_{AA}^{q,g}(P_f, \vec{x}_0, \phi) = \frac{g_0[P_0(P_f)]}{g_0(P_f)} \frac{dP_0^2}{dP_f^2}. \quad (4)$$

For our model specified by Eq. (1), the initial jet-parton momentum, $P_0(P_f)$, depends on the final quenched parton momentum P_f as [15]

$$P_0(P_f) = \left[P_f^{1-a} + K \int_{\tau_0}^{\tau_f} \tau^z T^{z-a+2}[\vec{x}_\perp(\tau), \tau] d\tau \right]^{\frac{1}{1-a}}, \quad (5)$$

where $K = \kappa C_2(1-a)/(\hbar c)^{1+z}$ and $C_2 = 3$ for gluon jets and $C_2 = 4/3$ for quark jets. Note that we could simulate non-monotonic density-dependent scenarios, as for example proposed in Ref. [37], by generalizing Eq. (5) and replacing $K \rightarrow K(\tau)$ inside the path integral. Here, we limit our applications to the simpler monotonic case.

After averaging over \vec{x}_0 , the pion nuclear modification factor $R_{AA}^\pi(p_\pi, \phi)$ is given by

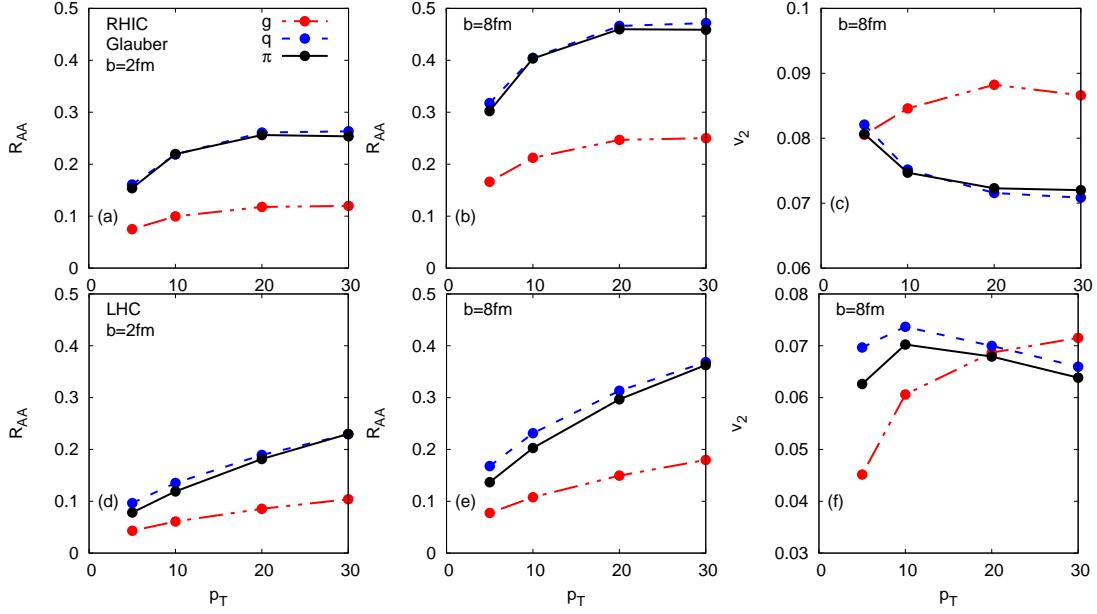


FIG. 1: (Color online) The R_{AA} and v_2 as a function of p_T for gluons (red dashed-dotted lines), quarks (blue dashed lines), and pions (black solid lines) at an impact parameter of $b = 2$ fm (left panel) and $b = 8$ fm (middle and right panel). A pQCD-like energy loss ($a = 1/3, z = 1$) with Glauber initial conditions is considered for RHIC $\sqrt{s} = 0.2$ ATeV with $\kappa = 0.93$ (upper panels) and extrapolated to LHC $\sqrt{s} = 2.76$ ATeV (lower panel) with a reduced coupling $\kappa = 0.66$ as discussed later in the text.

$$\begin{aligned}
 R_{AA}^{\pi}(p_{\pi}, \phi) &= \frac{d\sigma_q \otimes R_q \otimes D_{\pi/q} + d\sigma_g \otimes R_g \otimes D_{\pi/g}}{d\sigma_q \otimes D_{\pi/q} + d\sigma_g \otimes D_{\pi/g}} \\
 &= \frac{\sum_{\alpha=q,g} \int_{z_{min}}^1 \frac{dz}{z} d\sigma_{\alpha} \left(\frac{p_{\pi}}{z} \right) R_{AA}^{\alpha} \left(\frac{p_{\pi}}{z}, \phi \right) D_{\alpha \rightarrow \pi} \left(z, \frac{p_{\pi}}{z} \right)}{\sum_{\alpha=q,g} \int_{z_{min}}^1 \frac{dz}{z} d\sigma_{\alpha} \left(\frac{p_{\pi}}{z} \right) D_{\alpha \rightarrow \pi} \left(z, \frac{p_{\pi}}{z} \right)}, \quad (6)
 \end{aligned}$$

with $z_{min} = \frac{2p_{\pi}}{\sqrt{s}}$. Here we use the KKP pion fragmentation functions [44].

Figure 1 shows the R_{AA} and v_2 as a function of p_T for gluons (red dashed-dotted lines) and quarks (blue dashed lines) before fragmentation, as well as pions (black solid lines) after fragmentation for a pQCD-like energy loss and Glauber initial conditions. CGC-like conditions look very similar and are thus not shown here. The upper panel displays RHIC and the lower panel LHC energies where a reduced coupling was taken into account to fit the central 0-5% R_{AA} LHC data (see Fig. 5 and later discussion).

It can be seen from Fig. 1 that in case of RHIC energies (upper panel) the pion R_{AA}^{π} and v_2^{π} are dominated by quark jets because gluons are much more quenched and have softer fragmentation functions. Surprisingly, even at LHC energies (lower panel of Fig. 1), nuclear modifications of pions still follows closely the nuclear modification

of quark jets.

From the above calculated $R_{AA}^{\pi}(p_{\pi}, \phi) = R_{AA}^{\pi}(p_{\pi}, N_{part}, \phi)$ [see Eq. (6)], the $R_{AA}^{\pi}(N_{part})$ for a chosen $p_{\pi} = \text{const.}$ can be obtained by averaging over all possible angles ϕ [31]. The coupling constant κ is fixed such that it reproduces the value for R_{AA} in the most central collisions at RHIC energies. Then, the $v_n(p_T = \text{const.}, N_{part}) = v_n(N_{part})$ are computed via

$$v_n^{\pi}(N_{part}) = \frac{\int d\phi \cos \{n[\phi - \psi_n]\} R_{AA}^{\pi}(N_{part}, \phi)}{\int d\phi R_{AA}^{\pi}(N_{part}, \phi)}. \quad (7)$$

The Fourier density components e_n and the reaction-plane axis ψ_n are determined according to the initial density distribution used in Ref. [47]

$$e_n(t) = \frac{\sqrt{\langle r^2 \cos(n\phi) \rangle^2 + \langle r^2 \sin(n\phi) \rangle^2}}{\langle r^2 \rangle} \quad (8)$$

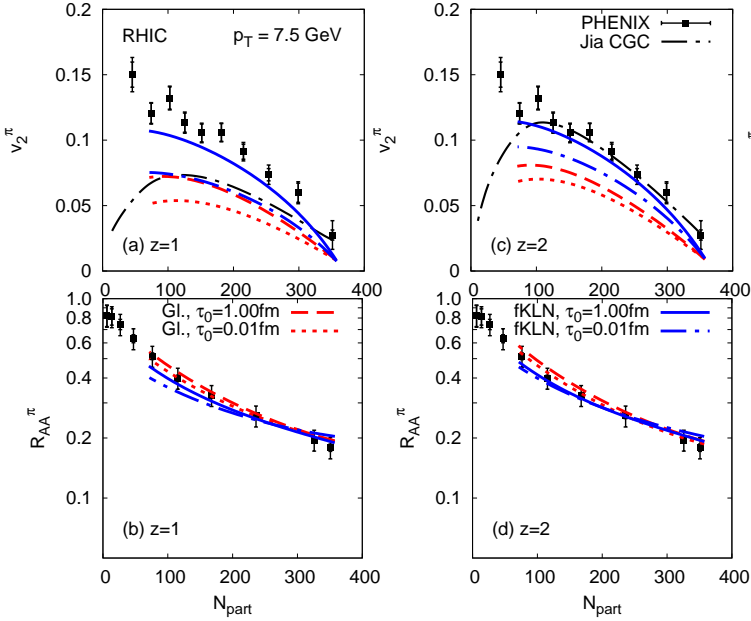


FIG. 2: (Color online) The $R_{AA}^{\pi}(N_{part})$ and the $v_2^{\pi}(N_{part})$ at RHIC energies after fragmentation for a pQCD-like energy loss ($z = 1$, left panel) as well as an AdS/CFT-like energy loss ($z = 2$, right panel). Glauber initial conditions are displayed by red lines, fKLN initial conditions by blue lines. The initialization times are either $\tau_0 = 1$ fm or $\tau_0 \sim 0$ fm. The black dashed-dotted line represents the result for CGC initial conditions taken from Ref. [34].

and

$$\psi_n(t) = \frac{1}{n} \tan^{-1} \frac{\langle r^2 \sin(n\phi) \rangle}{\langle r^2 \cos(n\phi) \rangle}. \quad (9)$$

By definition, the impact parameter points into the x -direction, but event-by-event fluctuations introduce non-trivial and harmonic dependent ψ_n 's.

To simulate Glauber initial conditions, we use a simple Monte Carlo model [31]. In case of the CGC initial conditions, we obtain initial conditions according to the Kharzeev-Levin-Nardi (KLN) model by deforming the Glauber initial conditions via

$$x_j \rightarrow x_j \sqrt{\frac{\langle x^2 \rangle_{\text{KLN}}}{\langle x^2 \rangle_{\text{Glauber}}}}, \quad (10)$$

with $\langle \circ \rangle$ denoting the average of a quantity.

The energy density (and thus temperature) is conserved due by assuming that

$$e(i, j) \rightarrow e(i, j) / \sqrt{\frac{\langle x^2 \rangle \langle y^2 \rangle_{\text{KLN}}}{\langle x^2 \rangle \langle y^2 \rangle_{\text{Glauber}}}}. \quad (11)$$

We checked that the temperature profiles and eccentricities of this azimuthally deformed Glauber model, henceforth referred to as fKLN, coincide with the ones of the fKLN model of Drescher et. al. [29, 30]. Since we showed

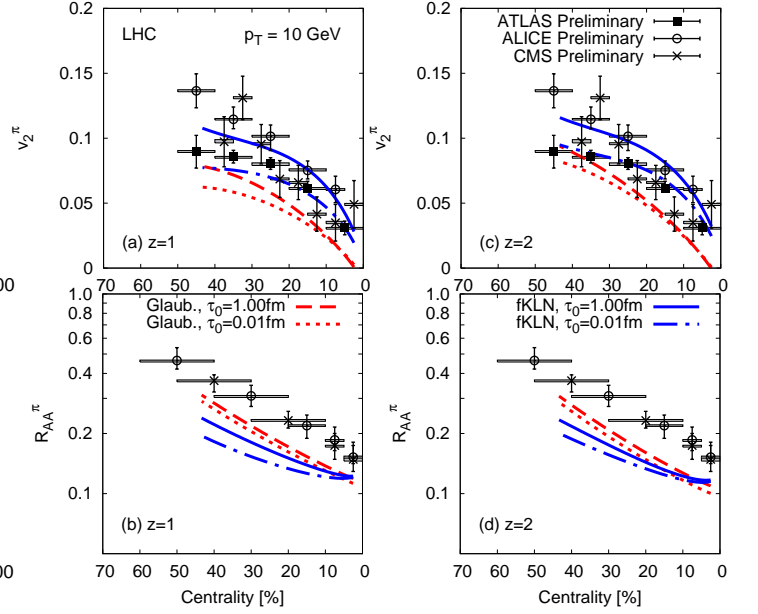


FIG. 3: (Color online) The $R_{AA}^{\pi}(\text{Centr.})$ and the $v_2^{\pi}(\text{Centr.})$ at LHC energies after fragmentation for a pQCD-like energy loss (left panel) as well as an AdS/CFT-like energy loss (right panel), assuming that the coupling constant κ does not change as compared to RHIC energies. The line coding is the same as in Fig. 2. The horizontal bars display the width of the centrality classes chosen by the different LHC collaborations. Data are taken from Refs. [10, 48–50].

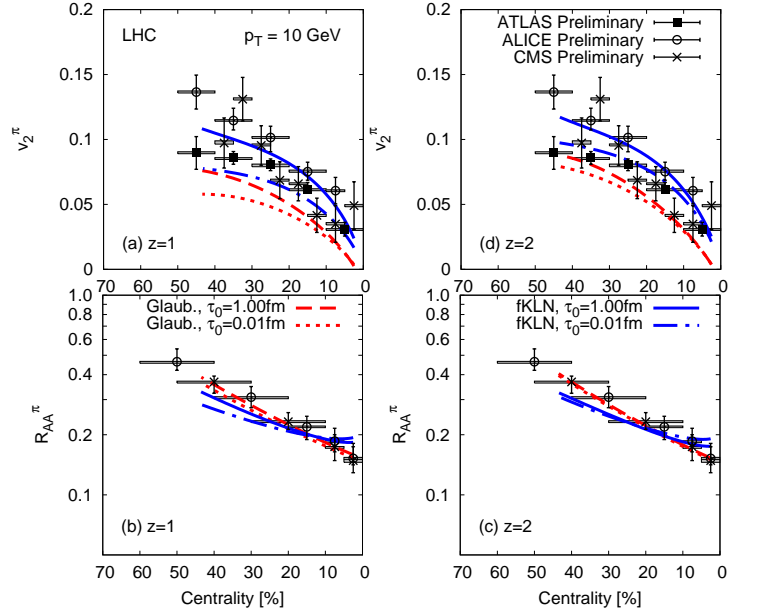


FIG. 4: (Color online) The $R_{AA}^{\pi}(\text{Centr.})$ and the $v_2^{\pi}(\text{Centr.})$ at LHC energies after fragmentation for a pQCD-like energy loss (left panel) as well as an AdS/CFT-like energy loss (right panel) for a reduced coupling constant. The line coding is the same as in Fig. 2. The horizontal bars display the width of the centrality classes chosen by the different LHC collaborations. Data are taken from Refs. [10, 48–50]. For fKLN initial conditions, κ is reduced such that the slope of the $R_{AA}^{\pi}(\text{Centr.})$ is better described.

in Ref. [31] that event-by-event geometrical fluctuations lead to very similar R_{AA} and v_2 as event-averaged geometries, we consider only the event-averaged geometries in this paper.

III. RESULTS AND DISCUSSION

Figure 2 shows the centrality dependence of $R_{AA}^\pi(N_{part})$ and the $v_2^\pi(N_{part})$ for pions at RHIC energies after fragmentation considering a pQCD-like energy loss (left panel) as well as an AdS/CFT-like energy loss (right panel) for Glauber initial conditions (red lines) or fKLN initial conditions (blue lines), and different initialization times $\tau_0 = 1$ fm or $\tau_0 \sim 0$ fm. As discussed in the introduction, we refer to a pQCD-like energy loss for $a = 1/3, z = 1$ and to an AdS/CFT-like energy loss for $a = 1/3, z = 2$.

The results are similar to those shown in Ref. [31] where the full convolution with initial spectra and pion fragmentation functions were only approximated. While the Glauber initial conditions and a small τ_0 fail to simultaneously describe the measured R_{AA} and v_2 data at RHIC [34], fKLN initial conditions and a $\tau_0 = 1$ fm gets close to these data for *both* a pQCD-like and an AdS/CFT-like energy loss.

Assuming that neither the coupling κ nor the initialization time τ_0 changes between RHIC to LHC initial conditions, we obtain the results shown in Fig. 3. Here, the R_{AA}^π and the v_2^π are displayed as a function of centrality classes like the data taken from Refs. [10, 48–50]. The line coding is the same as in Fig. 2. The horizontal bars display the width of the centrality classes chosen by the different LHC collaborations.

Fig. 3 clearly shows that the nuclear modification factor is underpredicted for both Glauber and fKLN initial conditions at LHC. This problem is common to all density-dependent energy-loss prescriptions [cf. Eq. (1)] as discussed in Refs. [15–17]. Note that v_2^π for the most central collisions is dominated by dynamical and finite number fluctuations that are not correctly treated in the event-averaged geometry used here. The fKLN initial conditions for a $\tau_0 = 1$ fm seem to reproduce the v_2 -data for both pQCD (left panel) and AdS/CFT-like energy loss (right panel). However, note that present large v_2 -data differences between ALICE, ATLAS, and CMS above 10 GeV remain to be resolved. This will be further emphasized below in connection with Fig. 7.

Since our results support the conclusion that the QGP created at LHC appears more transparent than expected based on fixed-coupling extrapolations from RHIC [15, 17], it is important to quantify the magnitude of the reduction needed to obtain Fig. 4. The ratio of the coupling needed to reproduce the LHC data to the one that fits RHIC data provides a measure of the degree of weakening of the effective jet-medium coupling as the QGP density doubles from RHIC to LHC under the assumption of a monotonic density-dependent energy

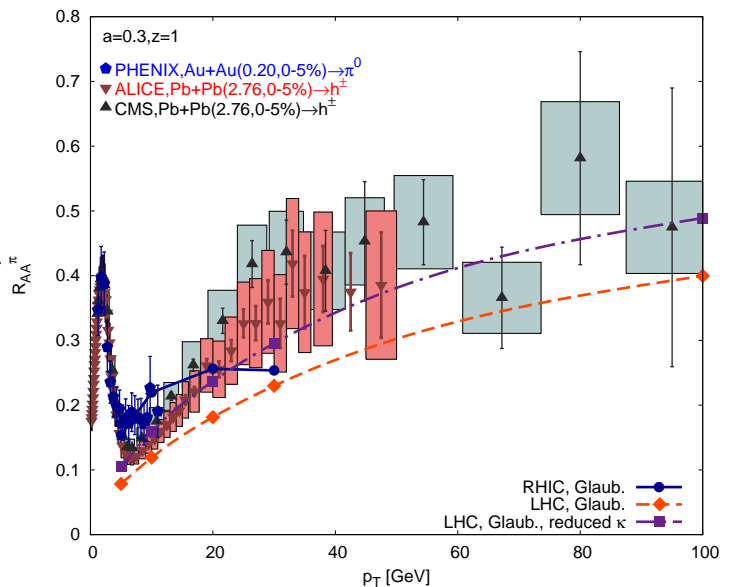


FIG. 5: (Color online) The nuclear modification factor of pions at 0–5% centrality as a function of p_T , shown for Glauber initial conditions, considering a pQCD-like energy loss ($z = 1$) at RHIC (blue circles) and LHC energies. Here, the orange diamonds represent the scenario where the coupling constant κ was held fixed at LHC as compared to RHIC energies, while the purple square display the results for a reduced coupling constant. The initialization time is chosen to be $\tau_0 = 1$ fm. The data are taken from Refs. [10, 48, 52].

loss.

In pQCD, $\kappa \propto \alpha^3$ leads to the approximate relation

$$\alpha_{\text{LHC}} = (\kappa_{\text{LHC}}/\kappa_{\text{RHIC}})^{1/3} \alpha_{\text{RHIC}}, \quad (12)$$

where $\alpha_{\text{RHIC}} \sim 0.3$. Inserting the values used in Figs. 3 and 4, which are summarized in Table I, we find that $\alpha_{\text{LHC}} \sim 0.24 - 0.27$, indicating a plausible moderate reduction of the pQCD coupling due to slow running (creeping) above the deconfinement temperature (see also Ref. [15–17]). Remarkably, by comparing Table I with Table II, we find that the ratio of LHC to RHIC effective couplings is insensitive to the assumed τ_0 in the range 0–1 fm/c.

On the other hand, in the falling-string scenario [38, 39, 41–43], the effective jet-medium coupling $\kappa \propto \sqrt{\lambda}$ is related to the square root of the t'Hooft coupling $\lambda = g_{YM}^2 N_c$. Gravity-dual descriptions require that $\lambda \gg 1$. For heavy-quark quenching, it was found in Ref. [25] that large $\lambda_{\text{RHIC}} \sim 20$ provides a reasonably good fit to the RHIC data as well as to the bulk v_2 elliptic flow.

In the falling string scenario, λ_{LHC} and λ_{RHIC} are then related via

$$\lambda_{\text{LHC}} = (\kappa_{\text{LHC}}/\kappa_{\text{RHIC}})^2 \lambda_{\text{RHIC}}. \quad (13)$$

From the holographic point of view, Tables I and II imply that λ_{LHC} must be reduced by a rather large factor of

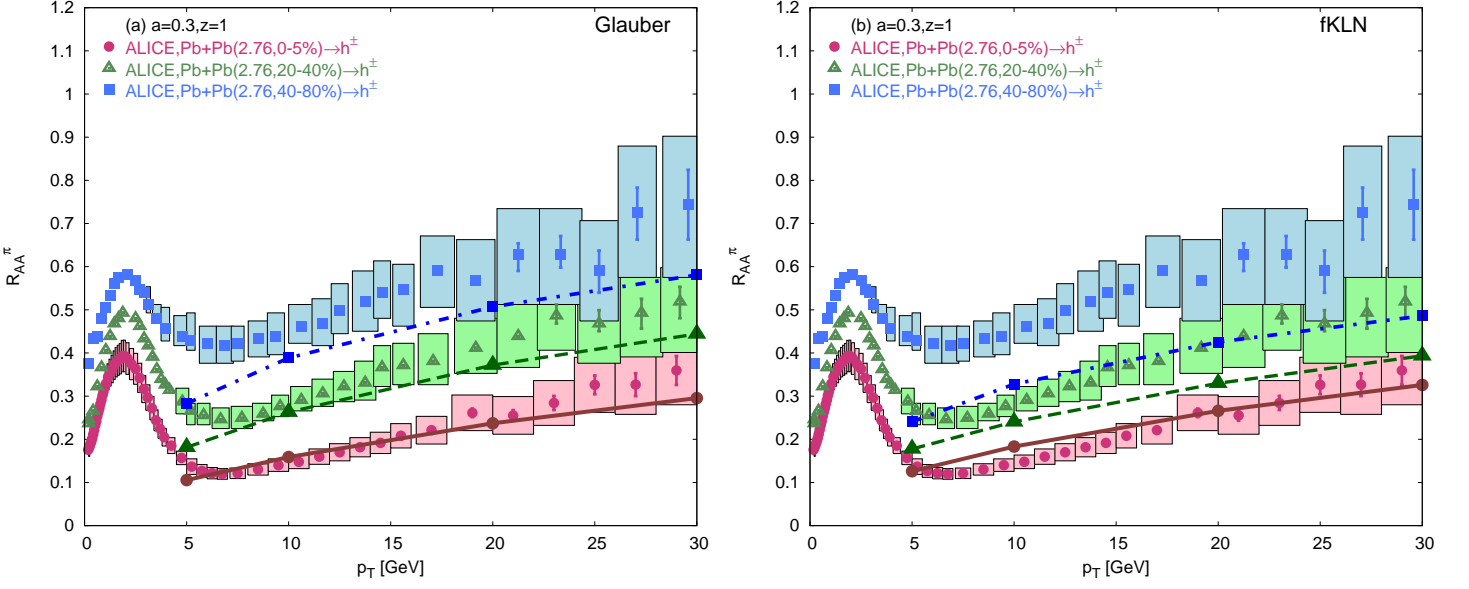


FIG. 6: (Color online) The nuclear modification factor of pions as a function of p_T for 0 – 5% (solid magenta line), 20 – 40% (dashed green line), and 40 – 80% (dashed-dotted blue line) centralities at LHC energies, compared to a pQCD-like energy loss scenario and either Glauber (left panel) or fKLN initial conditions (right panel), assuming a reduced coupling constant. The data are taken from Ref. [48].

$\sim 2 - 4$ relative to RHIC. This result implies a rather strong breaking of conformal symmetry over a narrow temperature interval. It is not yet clear if current non-conformal holographic models are consistent with such a strong variation (see, for example, Refs. [42, 51]).

Effective Coupling κ assuming $\tau_0 = 1.0$ fm/c				
\sqrt{s}	GL, $z=1$	fKLN, $z=1$	GL, $z=2$	fKLN, $z=2$
0.20	0.93	0.89	0.55	0.52
2.76	0.66	0.54	0.33	0.26
LHC/RHIC	0.71	0.61	0.60	0.50

TABLE I: The effective coupling κ at RHIC and LHC energies for Glauber and fKLN initial conditions and $\tau_0 = 1.0$ fm/c. The last row displays the ratio $\kappa_{LHC}/\kappa_{RHIC}$.

Effective Coupling κ assuming $\tau_0 = 0.01$ fm/c				
\sqrt{s}	GL, $z=1$	fKLN, $z=1$	GL, $z=2$	fKLN, $z=2$
0.20	0.60	0.54	0.44	0.37
2.76	0.45	0.33	0.26	0.18
LHC/RHIC	0.75	0.61	0.59	0.49

TABLE II: Same as table I but for fits assuming $\tau_0 = 0.01$ fm/c.

As Figs. 3 and 4 also reveal, the Glauber initial conditions describe the slope of the $R_{AA}^\pi(\text{Centr.})$ very well while the fKLN initial conditions show a different behavior. This effect will be discussed below. Moreover, there is hardly any difference between the pQCD-like and the AdS/CFT-like energy loss. Thus, we will omit the $dE/dx \sim l^2$ case in the following.

In a next step, we investigate the p_T -dependence of the R_{AA}^π and the v_2^π as displayed in Figs. 5 - 7.

While the RHIC data for most central collisions are well described for a pQCD-like energy loss (see Figs. 5) when $\tau_0 = 1$ fm, the LHC data are underpredicted if the coupling constant is not reduced (diamond symbols in Fig. 5). However, if one reduces κ as discussed above (the reference point is $p_T = 10$ GeV for most central collisions, see squares in Fig. 5), the energy-loss prescription follows the trend of the $R_{AA}^\pi(p_T)$ up until $p_T = 100$ GeV. Here, only Glauber initial conditions are displayed since fKLN initial conditions lead to similar results (see Fig. 4).

On the other hand, there is a difference in the $R_{AA}^\pi(p_T)$ for various centralities and initial conditions as Fig. 6 shows. For Glauber initial conditions (left panel), the centrality dependence is reproduced quite well while for fKLN initial conditions (right panel), the $R_{AA}^\pi(p_T)$ for larger centralities is underpredicted. The reason is that the temperatures in the fKLN approach need to be larger than for Glauber initial conditions in order to reproduce the same multiplicity. This larger temperatures lead to a larger energy loss according to Eq. (1) and thus a smaller $R_{AA}^\pi(p_T)$.

In case of the elliptic flow (cf. Fig. 7), any conclusion concerning the initial conditions strongly depend on the method chosen to extract the v_2^π from experimental data. Considering the event-plane method, as done by the ATLAS Collaboration (left panel of Fig. 7) [50], the fKLN initial conditions (lower panel) overpredict the data taken at LHC [49] while for Glauber initial conditions (upper panel), the results obtained are in quite good agreement with the present data in the 10 to 20 GeV range.

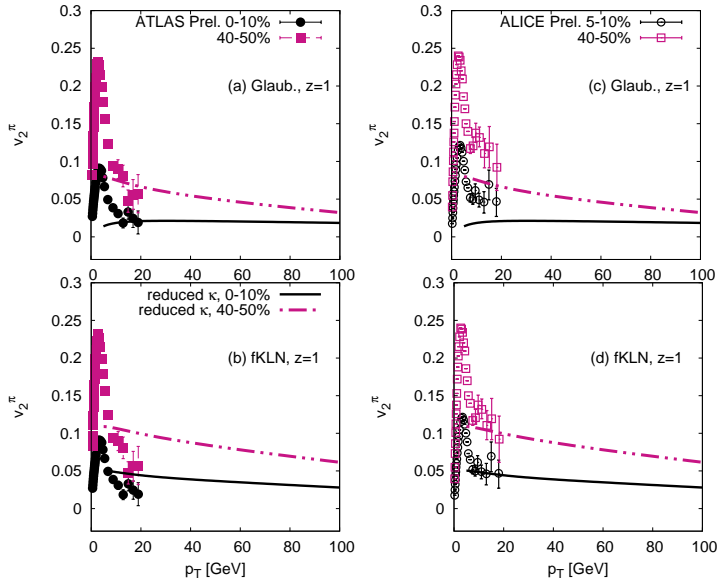


FIG. 7: (Color online) v_2^π as a function of p_T , shown for different centralities at LHC energies for a pQCD-like energy loss, compared to ATLAS (left panel, full symbols) and ALICE data (right panel, open symbols). Glauber initial conditions are displayed in the upper panel and fKLN initial conditions in the lower panel. The solid black and dashed-dotted magenta curves represent the results for a reduced coupling constant and different centralities at LHC energies. The initialization time is chosen to be $\tau_0 = 1$ fm. The data are taken from Refs. [49, 50].

Comparing, however, our results to the v_2^π -data obtained via two-particle correlations from the ALICE Collaboration [49] (right panel), the conclusion is reversed. fKLN initial conditions reproduce the ALICE v_2^π well while Glauber initial conditions underpredict those data. The difference in the data sets may be due to non-flow effects included in the ALICE data. Obviously, firmer conclusions will require reduced discrepancies between the data sets. Future v_2^π data extending up to $10 < p_T \sim 100$ GeV at LHC as predicted in Fig. 7, can provide even more stringent test for jet-medium interactions. For our pQCD-like model the elliptic moment for central collisions is predicted to stay flat up to $p_T = 100$ GeV while v_2^π for more peripheral collisions is predicted to decrease slowly approaching the value for central collisions.

IV. SUMMARY

Using a generic power-law model of energy, path-length and monotonic density-dependent energy-loss with KKP fragmentation, we found that the pion nuclear modification factor R_{AA}^π and elliptic flow v_2^π at RHIC can be described by *either* a linear, pQCD-like *or* a quadratic, AdS/CFT-like energy-loss model if the initialization time

is assumed to be $\tau_0 = 1$ fm, as preferred from hydrodynamic fits to the bulk elliptic flow systematics [46], and choosing a fKLN/CGC initial geometry as also required for consistency with bulk low- p_T QGP elliptic flow at RHIC [31–33].

Our monotonic density-dependent energy-loss model predicts overquenching of R_{AA}^π at LHC similar to previous RHIC-constrained jet-tomography extrapolation [15–17]. We showed that a moderate reduction of the effective jet-medium coupling at LHC with $\alpha_{LHC} \sim 0.24 - 0.27$ relative to RHIC ($\alpha_{RHIC} = 0.3$) can account for both, the measured R_{AA}^π and v_2^π -data at LHC.

In terms of strongly-coupled holographic models, however, our LHC fit requires a much larger reduction of the effective t'Hooft coupling from $\lambda_{RHIC} \sim 20$ by a factor of 2 – 4 to $\lambda_{LHC} \sim 5 - 10$. This suggests stronger non-conformal effects that must be considered for a holographic phenomenology of LHC.

Surprisingly, we found that fKLN/CGC initial conditions appear to fail describing the centrality dependence of the $R_{AA}^\pi(p_T)$ and $v_2^\pi(p_T)$ at LHC energies. This is in contrast to RHIC energies, where fKLN is preferred. At LHC energies, a pQCD-like energy loss with Glauber initial conditions seem to provide the best simultaneous description of the p_T and centrality dependence of these two single-hadron measures of jet-medium interactions.

As demonstrated in Fig. 1, the nuclear modification factor as well as the elliptic moment at both RHIC and LHC energies for $p_T > 5$ GeV are dominated by quark jet-quenching and fragmentation because gluon jets are strongly quenched and fragmentation leads to pions with a smaller fractional momentum. This underlines the conclusion of Ref. [17] that single-hadron jet-flavor tomography observables are mainly sensitive to quark rather than gluon jet-medium interactions. The reduced jet-medium coupling quantified in this work therefore refers primarily to the apparent weakening of quark-jet interactions in a QGP when the density approximately doubles from RHIC to LHC. It remains a challenge to identify jet observables more sensitive to gluon jet-quenching to test color Casimir scaling currently assumed in both weakly-coupled pQCD tomography and strongly-coupled string holography. Di-hadron and jet-shape observables could help to probe gluon versus quark jet-medium interactions in the future.

Acknowledgments

B.B. is supported by the Alexander von Humboldt foundation via a Feodor Lynen fellowship. M.G. and B.B. acknowledge support from DOE under Grant No. DE-FG02-93ER40764. The authors thank G. Torrieri, J. Jia, A. Buzzatti, A. Ficnar, W. Horowitz, J. Liao, M. Mia, J. Noronha, J. Harris, G. Roland, B. Cole, and W. Zajc for extensive and fruitful discussions.

-
- [1] K. Aamodt [ALICE Collaboration], Phys. Lett. B **696**, 30 (2011).
 - [2] J. Otwinowski [ALICE Collaboration], J. Phys. G G **38**, 124112 (2011).
 - [3] H. Appelshauser and f. t. A. Collaboration, J. Phys. G G **38**, 124014 (2011).
 - [4] G. C. B. f. t. A. collaboration, J. Phys. G G **38**, 124117 (2011).
 - [5] J. Schukraft and f. t. A. Collaboration, J. Phys. G G **38**, 124003 (2011).
 - [6] A. Dainese and f. t. A. Collaboration, J. Phys. G G **38**, 124032 (2011).
 - [7] [ATLAS Collaboration], arXiv:1108.6027 [hep-ex].
 - [8] P. Steinberg and A. Collaboration, J. Phys. G G **38**, 124004 (2011).
 - [9] J. J. f. t. A. Collaboration, J. Phys. G G **38**, 124012 (2011).
 - [10] CMS Collaboration, Physics Analysis Summary (PAS), <http://cdsweb.cern.ch/record/1347788?ln=en>.
 - [11] A. S. Y. f. t. C. collaboration, arXiv:1107.1862 [nucl-ex].
 - [12] S. Chatrchyan *et al.* [CMS Collaboration], JHEP **1108**, 141 (2011).
 - [13] S. Chatrchyan *et al.* [CMS Collaboration], JHEP **1107**, 076 (2011).
 - [14] S. Chatrchyan *et al.* [CMS Collaboration], Phys. Rev. C **84**, 024906 (2011).
 - [15] W. A. Horowitz and M. Gyulassy, Nucl. Phys. A **872** (2011) 265.
 - [16] B. G. Zakharov, JETP Lett. **93**, 683 (2011).
 - [17] A. Buzzatti and M. Gyulassy, Phys. Rev. Lett. in press, arXiv:1106.3061 [hep-ph].
 - [18] I. Vitev, J. Phys. G G **38**, 124087 (2011).
 - [19] M. Gyulassy and L. McLerran, Nucl. Phys. A **750**, 30 (2005); E. V. Shuryak, Nucl. Phys. A **750**, 64 (2005).
 - [20] I. Arsene *et al.* [BRAHMS Collaboration], Nucl. Phys. A **757**, 1 (2005).
 - [21] B. B. Back *et al.*, Nucl. Phys. A **757**, 28 (2005).
 - [22] J. Adams *et al.* [STAR Collaboration], Nucl. Phys. A **757**, 102 (2005).
 - [23] K. Adcox *et al.* [PHENIX Collaboration], Nucl. Phys. A **757**, 184 (2005).
 - [24] J. M. Maldacena, Adv. Theor. Math. Phys. **2**, 231-252 (1998).
 - [25] J. Noronha, M. Gyulassy and G. Torrieri, Phys. Rev. C **82**, 054903 (2010).
 - [26] M. L. Miller, K. Reygers, S. J. Sanders and P. Steinberg, Ann. Rev. Nucl. Part. Sci. **57**, 205 (2007).
 - [27] E. Iancu and R. Venugopalan, arXiv:hep-ph/0303204.
 - [28] D. Kharzeev and E. Levin, Phys. Lett. B **523**, 79 (2001).
 - [29] H. J. Drescher, A. Dumitru, C. Gombeaud and J. Y. Ollitrault, Phys. Rev. C **76**, 024905 (2007).
 - [30] H. J. Drescher, A. Dumitru, A. Hayashigaki and Y. Nara, Phys. Rev. C **74**, 044905 (2006).
 - [31] B. Betz, M. Gyulassy, G. Torrieri, Phys. Rev. C **84**, 024913 (2011).
 - [32] B. Betz, M. Gyulassy and G. Torrieri, J. Phys. G G **38**, 124153 (2011).
 - [33] A. Drees, H. Feng and J. Jia, Phys. Rev. C **71**, 034909 (2005); J. Jia and R. Wei, Phys. Rev. C **82**, 024902 (2010).
 - [34] A. Adare *et al.* [PHENIX Collaboration], Phys. Rev. Lett. **105**, 142301 (2010).
 - [35] J. Jia, W. A. Horowitz and J. Liao, Phys. Rev. C **84**, 034904 (2011).
 - [36] R. J. Fries and R. Rodriguez, Nucl. Phys. A **855**, 424 (2011).
 - [37] J. Liao, arXiv:1109.0271 [nucl-th]; J. Liao and E. Shuryak, Phys. Rev. Lett. **102**, 202302 (2009).
 - [38] S. S. Gubser, D. R. Gulotta, S. S. Pufu and F. D. Rocha, JHEP **0810**, 052 (2008).
 - [39] P. M. Chesler, K. Jensen, A. Karch and L. G. Yaffe, Phys. Rev. D **79**, 125015 (2009).
 - [40] P. M. Chesler, K. Jensen and A. Karch, Phys. Rev. D **79**, 025021 (2009).
 - [41] P. Arnold and D. Vaman, JHEP **1104**, 027 (2011).
 - [42] A. Ficnar, J. Noronha and M. Gyulassy, J. Phys. G G **38**, 124176 (2011); Nucl. Phys. A **855**, 372 (2011).
 - [43] A. Ficnar, arXiv:1201.1780 [hep-th].
 - [44] B. A. Kniehl, G. Kramer and B. Potter, Nucl. Phys. B **597**, 337 (2001).
 - [45] J. D. Bjorken, Phys. Rev. D **27**, 140 (1983).
 - [46] H. Song, S. A. Bass, U. Heinz, T. Hirano and C. Shen, Phys. Rev. Lett. **106**, 192301 (2011).
 - [47] B. Alver and G. Roland, Phys. Rev. C **81**, 054905 (2010).
 - [48] H. Appelshauser and f. t. A. Collaboration, J. Phys. G G **38**, 124014 (2011).
 - [49] R. S. f. t. A. Collaboration, J. Phys. G G **38**, 124013 (2011).
 - [50] J. J. f. t. A. Collaboration, J. Phys. G G **38**, 124012 (2011).
 - [51] M. Mia, K. Dasgupta, C. Gale and S. Jeon, arXiv:1108.0684 [hep-th]; M. Mia and C. Gale, Nucl. Phys. A **830**, 303C (2009).
 - [52] A. Adare *et al.* [PHENIX Collaboration], Phys. Rev. Lett. **101**, 232301 (2008).